

Temperature Distribution in the Corona from λ 5303 Å Line-width Observations : Eclipse of 1980 February 16 – Tentative Evidence for a Temperature Maximum

J. N. Desai and T. Chandrasekhar

Physical Research Laboratory, Ahmedabad 380009

Received 1982 December 10; accepted 1983 March 23

Abstract. Fabry-Perot interferometric observations in the green coronal line during the total eclipse of 1980 February 16, have yielded line-width temperatures up to $1.5 R_{\odot}$ over a wide range of position angles. Least square analysis of the data indicates a tentative temperature maximum near $1.2 R_{\odot}$ from the centre of the Sun. The ratio of peak line intensity to square of the continuum intensity $E_{\text{line}}/E_{\text{cont}}^2$ appears to be inversely correlated to the temperature. Turbulent velocities calculated using this ratio and the observed line-width temperatures show a peak at $\sim 10 \text{ km s}^{-1}$.

Key words: solar corona – 1 5303 Å line widths – solar eclipse

1. Introduction

The location of a temperature maximum in the solar corona has important implications for coronal heating mechanisms (Kuperus 1969; Kopp & Orrall 1976; Brandt, Richard & Cassinelli 1965). The temperature structure of the inner corona, unlike the electron density distribution, is very poorly known mainly because of observational difficulties. Kuperus (1969) has reviewed theoretical coronal studies and finds some agreement for the temperature maximum to be located near $1.1 R_{\odot}$. Barne *et al.* (1974), from their examination of ion abundances in solar wind, find a negative temperature gradient even at $1.5 R_{\odot}$. Nakada *et al.* (1976) from a study of brightness gradients of extreme ultraviolet (EUV) lines measured with OSO-7 conclude that the negative temperature gradient may extend to as low as $1.2 R_{\odot}$. On the other hand Mariska & Withbroe (1978), from a similar study conducted from Skylab, find evidence for a positive temperature gradient from 1.03 to $1.23 R_{\odot}$. They suggest a temperature maximum at $\sim 1.3 R_{\odot}$. Kohl *et al.* (1980) obtained resonant scattered Lyman α profiles from a rocket experiment and find a steady decrease in the widths from

2.5×10^6 K at $2 R_{\odot}$ to 1.0×10^6 K at $4 R_{\odot}$. Taking into account the earlier observations of Mariska & Withbroe (1978), these authors deduce the maximum temperature of the solar corona to be 2.5×10^6 K and locate it between $1.5 R_{\odot}$ and $2.0 R_{\odot}$. In this paper evidence is presented for a tentative temperature maximum at $1.2 \pm 0.05 R_{\odot}$ from the solar centre from interferometric line-width observations of the green coronal line taken during the total solar eclipse of February 16, 1980.

2. Observations

Details of the instrumentation used, observations made and preliminary results are reported elsewhere (Chandrasekhar *et al* 1980; Chandrasekhar, Desai & Angreji 1981; Desai, Chandrasekhar & Angreji 1982). Essentially an air-spaced optically-contacted etalon was coupled to a telescope-coelostat set up to obtain during totality, green line fringes off-centred with respect to the centre of the solar disk. The optically contacted Fabry-Perot etalon is a relatively new development in the field of interferometry. Details of the technique are given in Smartt & Ramsay (1964) and in Bates *et al.* (1966). Essentially, in this type of etalon, the traditional spacers are replaced by optically flat quartz pieces whose thicknesses are equal within 1/100th of the wavelength of visible light. The close contact between the quartz pieces and the plates allows molecular forces to form a bond and keeps the etalon in permanent alignment. Such a stable Fabry-Perot etalon is especially suited for field observations such as an eclipse.

Immediately after totality, the interferometer was calibrated using a spectral lamp in the green line of mercury (λ 15460.74 Å). The calibration frame and the four eclipse frames were scanned in a Carl Zeiss microdensitometer with a slit area corresponding to 13 arcsec \times 6 arcsec in the plane of the sky. Since the green line, during this eclipse, was much stronger than the continuum ($E_{\text{line}}/E_{\text{cont}} > 10$) in the 7-Å band-width filter used, the fringes had a high contrast and were of good microphotometric quality. Fringes could be traced up to $1.5 R_{\odot}$ along many position angles. The continuum intensity at λ 5303 Å was calculated from the residual intensity midway between the fringes. The mean value of this intensity on either side of the fringe was taken as the continuum contribution (E_{cont}) for that fringe. The fringe peak value corrected for this continuum was taken as the true line intensity E_{line} and used in the calculation of a useful ratio $E_{\text{line}}/E_{\text{cont}}^2$.

Detailed microdensitometric analysis resulted in ~ 300 line-widths for the 90-s exposure frame spread over 37 scans made radially outward from the fringe centre. The temperatures are deduced from these line-widths assuming a pure thermal broadening. Out of the 37 scans, in the 24 scans which permitted adequate radial coverage, a temperature maximum is evident. In the remaining 13 scans the radial coverage of temperatures is insufficient to locate any maximum value. Due to difficulties in measuring the low value of the continuum intensity (E_{cont}), the ratio $E_{\text{line}}/(E_{\text{cont}}^2)$ could be evaluated with reasonable accuracy only for 10 of these 24 scans. These 10 scans comprising of about 60 values of the temperature and the ratio $E_{\text{line}}/(E_{\text{cont}}^2)$ are considered for detailed analysis.

3. Instrumental performance and sources of error

3.1 Microdensitometric Errors

The accuracy of line-width temperature measurements from the coronal interferogram is limited mainly by the grain noise of the film used. The most sensitive

parameter in the microdensitometric analysis is the depth or fringe maximum. Changing this parameter by an amount corresponding to the grain noise, one can evaluate the errors in line-width temperature measurements. It has been found that for fringes with good contrast ($E_{\text{line}}/E_{\text{cont}} > 10$), The temperature could be determined accurate to ± 10 per cent. For fringes with lower contrast the accuracy was correspondingly lower $\sim \pm 25$ per cent. In this analysis only fringes with good contrast are considered. The data sample was further restricted to 60 fringes by the necessity of measuring $E_{\text{line}}/E_{\text{cont}}^2$ to the derived accuracy of ± 10 per cent.

3.2 Tracking Errors

Due to the inaccurate tracking of the coelostat, there has been a slight drift of the coronal image on the film. This smearing effect has been quantitatively evaluated by considering the separation of the fringe centre and the solar centre in the 3 exposures made during totality. In case of perfect tracking the separation would remain constant for all exposures. The systematic reduction in the separation indicates a drift corresponding to $0.084 R_{\odot}$ during the 90 s exposure. The smearing thus limits the achievable spatial resolution to $\sim \pm 0,04R_{\odot}$.

3.3 Focussing

The focus of the optical system was checked both just before and immediately after totality, and found to be satisfactory. It is therefore reasonable to expect the focusing to have been proper during the totality exposures.

3.4 Masking Effect

The coronal fringes are not seen in the region of position angles 100–200 deg. This is due to two effects: (i) Image drift in the focal plane and a cut-off in the portion by the entrance aperture, (ii) The off-centred position of the Fabry-Perot fringe system relative to the solar centre. The off-centring was done with the specific intention of obtaining fringe widths radially (from the solar centre) in some position angles and for reducing the fringe separation (and hence for improving spatial resolution) in other position angles. A few fringes in this zone have been lost due to the cut-off by the entrance aperture; but due to the fringe centre offset in this direction this number is small compared to the total number of fringes scanned. Apart from a marginal reduction in the number of fringes available for study, this effect has no bearing on the conclusions drawn.

3.5 Etalon Performance

The interferometer was calibrated using a low-pressure mercury lamp at $\lambda 5461\text{\AA}$ immediately after totality. The calibration interferogram was carefully studied to check the performance of the interferometer. An effective finesse value of ~ 20 and an instrumental resolution of 0.23\AA were obtained in excellent agreement with the manufacturer's quoted value, proving thereby that the etalon performance was perfect.

4. Results

Line-width temperatures are displayed in Figs 1 (a) and (b) as a function of projected radial distance for 10 scans in which a temperature maximum is evident. The mean position angle of the scan is also listed.

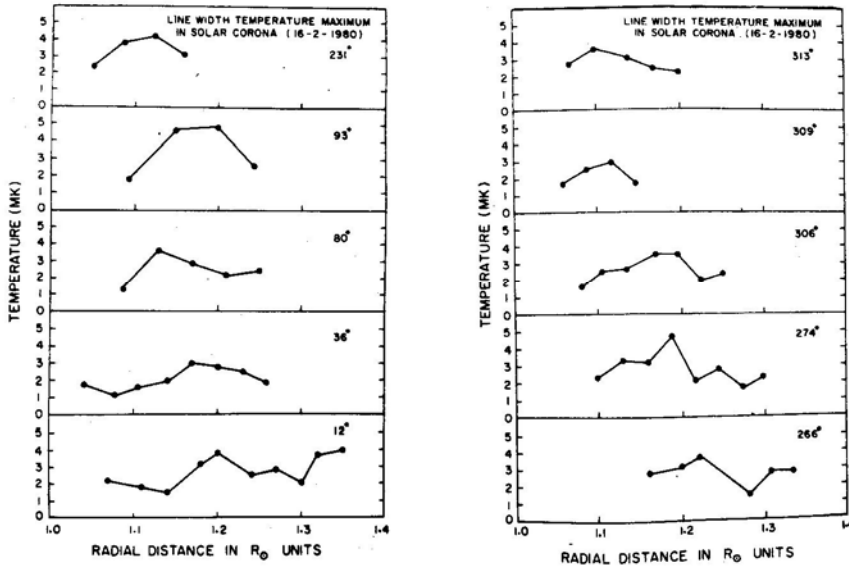


Figure 1. Line-width temperatures plotted against projected radial distance for different position angles (90-s interferogram). Estimated error in temperature measurement (best profiles): $\Delta T/T \sim \pm 0.1$.

The temperature peaks as seen in Fig. 1 appear to be located, except in one case, in the region $1.1 R_{\odot}$ to $1.2 R_{\odot}$. The exact location of the peak as well as the value of the maximum temperature is different for each scan. There appears to be no correlation between the value of the peak temperature and the position (R/R_{\odot}) at which it is observed.

5. Discussion

We have attempted to establish the existence of a temperature maximum statistically by considering the goodness of fit for the data of three representative curves – linear, quadratic and cubic. In addition to the normal analysis (case 1) two control situations (case 2 and case 3) are also considered. The goodness of fit has been evaluated by a χ^2 test and also by a comparison of correlation coefficients. Table 1 lists the correlation coefficients, the χ^2 values, the degrees of freedom in the three cases, and the radial distance at which the temperature reaches a maximum for the quadratic and cubic curves.

The correlation coefficients are small in all cases. This is to be expected as the line-width temperature distribution is not expected to vary in a simplistic linear, quadratic or cubic fashion. However what is of importance is the relative goodness of fit among the three curves. A better goodness of fit for the higher order curves indicates the possible existence of a temperature maximum. The correlation coefficients for the quadratic and cubic curves are statistically significant at the 5 per cent level, *i.e.* they have a probability of ≤ 0.05 of occurring by chance. The linear hypothesis is rejected at this level of significance. The correlation coefficients indicate in all cases that the goodness of fit is better for the quadratic and cubic than for the linear fit thereby indicating the existence of a real temperature maximum. These curves also show $d^2 T/dR^2 < 0$ at

the turning points *i.e.* maxima. The maximum temperature occurs at $1.25 R_{\odot}$ for the quadratic and $1.23 R_{\odot}$ for the cubic curve (case 1). A χ^2 test has also been performed on the data to test the goodness of fit with respect to linear, quadratic and cubic curves, along the lines outlined in Brandt (1970). The χ^2 statistic used is

$$\chi^2 = \sum_{j=1}^{\nu} \varepsilon_j / \sigma_j^2$$

where ε_j is the deviation of the observed value from the calculated value on the basis of linear, quadratic or cubic hypothesis and σ_j is the standard deviation. The summation is over the degrees of freedom which are slightly different for the hypotheses because of the different number of evaluated constants. The χ^2 value along with the degree of freedom ν in each case has also been listed in Table 1. It is seen that in all the 3 cases, χ^2 values for quadratic and cubic curves are lower compared to the linear value. In case 2 where all the temperatures in a scan are normalised to the peak value in that scan, the linear hypothesis would be rejected at the 5 per cent significance level but not quadratic or cubic hypotheses. Among the quadratic and cubic curves the fit seems better for the quadratic than the cubic curve.

Case 2 indicates a data set in which the temperatures measured radially along a position angle have been normalised with respect to the maximum temperature for the same position angle. The normalisation was intended to remove discrepancies in the curve-fitting procedure caused by the temperatures in different regions being markedly different. The temperature maximum for the quadratic fit is at $1.22 R_{\odot}$ though for the cubic the value has shifted to $1.35 R_{\odot}$.

In the above discussion, it is presumed that the temperature maximum is located at the same radial distance in different azimuths. An azimuthally asymmetric heat input could, however, cause the maxima to be located at somewhat different radial distances in different directions. One would then like to verify whether along any

Table 1. Results of statistical analysis.

	Case 1	Case 2	Case 3
<i>Linear</i>			
Correlation coefficient	0.210	0.152	0.117
ν	59	59	57
χ^2	96.64	79.53	105.13
<i>Quadratic</i>			
Correlation coefficient	0.28	0.24	0.30
ν	58	58	56
χ^2	90.50	76.10	87.93
Temperature maximum (R/R_{\odot})	1.25	1.22	1.18
<i>Cubic</i>			
Correlation coefficient	0.297	0.250	0.30
ν	57	57	55
χ^2	91.11	76.11	89.50
Temperature maximum (R/R_{\odot})	1.23	1.35	1.18

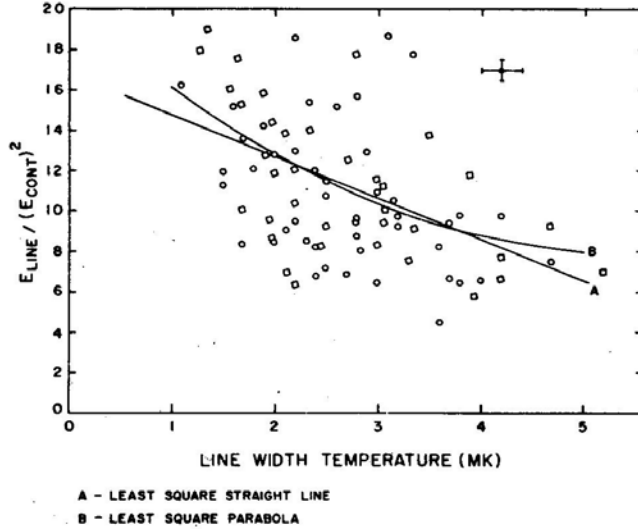


Figure 2. $E_{\text{line}}/E_{\text{cont}}^2$ plotted against line-width temperatures. A: linear fit with a correlation coefficient of 0.52; B: quadratic fit with a correlation coefficient 0.53.

particular direction in general the coronal temperature rises to a maximum and then drops. In order to do this, we have normalised the 10 radial plots of the temperature such that the apparent temperature maximum falls at $1.5 R_{\odot}$ for all directions. Correlation coefficients and χ^2 values for this analysis are tabulated under case 3. Case 3 has been included mainly to show the consistency in the analysis. The quadratic and cubic correlation coefficients are 2.5 times the linear correlation coefficient. The χ^2 test also favours the higher curves over the linear one. We are led to the conclusion on the basis of correlation coefficients and the χ^2 test that in any direction, in general, the coronal temperature rises to a maximum and then drops and that the region of maximum temperature is located at $1.2 \pm 0.05 R_{\odot}$.

So far in this analysis the excess broadening effect due to turbulence has not been considered. However, an indirect approach has been adopted to check on the temperature maximum. Figs 3(a) and (b) show the ratio of peak line intensity (E_{line}) to the square of the continuum intensity (E_{cont}) displayed as a function of radial distance from the centre of the solar disk. For a collisionally-excited line emission in an isothermal corona $E_{\text{line}} \propto N_c^2$ and since $E_{\text{cont}} \propto N_e$ the ratio $E_{\text{line}}/E_{\text{cont}}^2$ is expected to be approximately a constant. This ratio can be estimated from our observations with an accuracy of about 10 per cent. Departures of the ratio from constancy indicate real changes in ionisation temperatures as indicated by Liebenberg, Bessey & Watson (1975). For temperature above the temperature for the maximum population of the ion, $T = 2.0$ MK as given by Jordan (1969), the ratio $E_{\text{line}}/E_{\text{cont}}^2$ should go through a minimum as the temperature passes through a peak value. A point-by-point comparison of line-width temperatures and the ratio (Fig. 2) shows this inverse correlation. A least-square straight line and parabola fitted to the data are also shown. The correlation coefficient in both cases is 0.53 which is statistically significant even at the 1 per cent level, *i. e.* there is less than 1 per cent probability of it occurring by pure chance. This negative correlation between the ratio and line-width temperature indicates that though

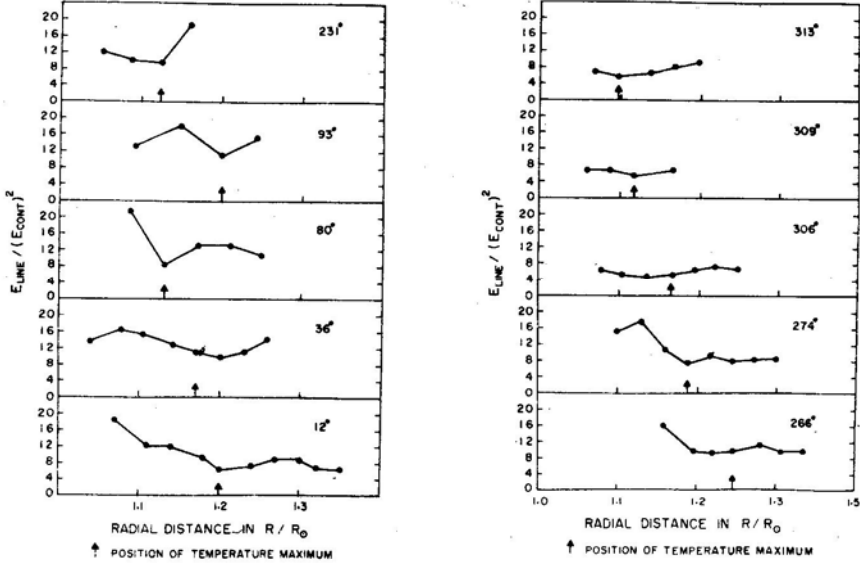


Figure 3. $E_{\text{line}}/E_{\text{cont}}^2$ plotted against projected radial distance for different position angles. Estimated percentage error $\sim \pm 10$ per cent.

the observed values of temperature may be higher than actual kinetic temperatures due to turbulence broadening, the observed phenomenon of temperature maximum and position of peak temperature are preserved unchanged.

Plots of $E_{\text{line}}/E_{\text{cont}}^2$ (Fig. 3), though slightly inferior in quality compared to the temperature values, (due to difficulties in measuring the low continuum level) nevertheless show a minimum at or close to the temperature maximum. The line-width temperature maximum positions are indicated by arrows (Fig. 3). A least-squares analysis for this ratio, similar to the one outlined for the temperature plots has been carried out. The χ^2 test does not distinguish between linear, quadratic and cubic curves for this ratio giving the same value of 74.9 in all three cases. However, the goodness of fit for higher order curves as determined by the ratio of correlation coefficients is better than for the linear case (~ 1.3 times) and the results yield a minimum value of the ratio at $1.23 R_{\odot}$ in reasonable agreement with the location of temperature maximum.

As a natural follow-up of the analysis we have evaluated the turbulent velocity distribution from the line-width temperature and the $E_{\text{line}}/E_{\text{cont}}^2$ values in the following manner. According to Dollfus (1971) the emission line intensity (E_{line}) can be written as

$$E_{\text{line}} = \frac{K_1 \exp(-W/kT_i)}{\sqrt{T_i}} \left(\frac{N_i}{N_0} \right) N_c^\alpha$$

where W is the excitation potential for the line ($W = 2.34$ eV for the green line). N_i/N_0 is the fraction of Fe xiv ions to the total number of iron atoms and is a strong function of temperature. For a collisionally-excited line such as the green line we can take

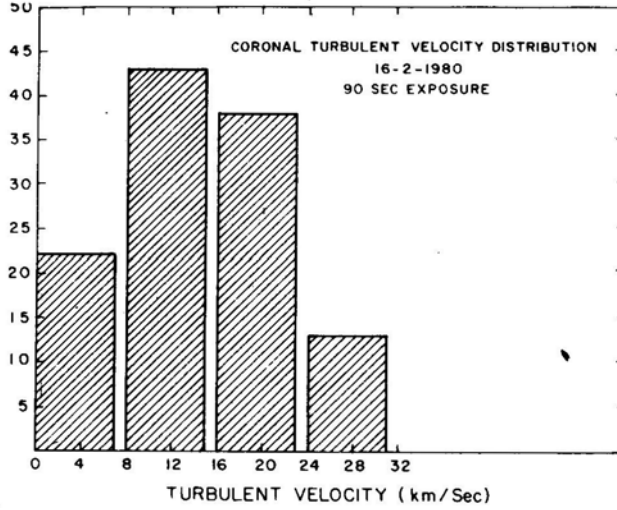


Figure 4. Histogram of turbulent velocities (90-s interferogram).

$\alpha = 2$. Writing the continuum intensity as $E_{\text{cont}} = K_2 N_e$ it is seen that

$$\frac{E_{\text{line}}}{E_{\text{cont}}^2} = K_3 \exp(-W/kT) \left(\frac{N_i}{N_0} \right) \frac{1}{\sqrt{T_i}}.$$

The ratio is independent of electron density N_e . Here, K_1 , K_2 and K_3 are constants; T_i is the ionisation temperature.

In the region of temperatures above the maximum population of the ion, the above expression simplifies to

$$\frac{E_{\text{line}}}{E_{\text{cont}}^2} \propto \frac{1}{T_i \beta}.$$

As evaluated from an ionisation curve (Jordan 1969), β has a value of 7.6429. The normalisation condition that the highest observed $E_{\text{line}}/E_{\text{cont}}^2$ (~ 31) occurs for the temperature of maximum abundance for the Fe XIV ion results in the expression

$$\log(E_{\text{line}}/E_{\text{cont}}^2) = -7.6429 \log T_i + 49.55.$$

Thus, knowing $E_{\text{line}}/E_{\text{cont}}^2$, one can calculate T_i and, hence, evaluate the turbulent velocity V_{turb} from the relation

$$V_{\text{turb}}^2 + \frac{2kT_i}{m} = \frac{2kT_D}{m}$$

where T_D is the line-width temperature, k is the Boltzmann constant and m is the mass number of the atom emitting the line ($= 56$ in our case).

The resulting turbulent velocity histogram is shown in Fig. 4. It shows a dominant

peak in the region 8–15 km s⁻¹. Interestingly a turbulent velocity of ~ 10 km s⁻¹ results in a temperature difference between T_D and T_i of $\sim 3 \times 10^5$ K which is about the right amount to account for the still persistent discrepancy between the two temperatures. The radial variation of turbulent velocities does not show any systematic trends particularly a decrease as noted in an earlier eclipse (Liebenberg, Bessey & Watson 1975).

6. Conclusion

Fabry-Perot interferometric observations of the green line during the total solar eclipse of 1980 February 16 have yielded line-width temperatures over a wide range of position angles. A least-square analysis and a χ^2 test performed on the data show that line-width temperatures tend to peak at a projected radial distance (as measured from the centre of the disk) of $1.2 \pm 0.05 R_\odot$. The ratio $E_{\text{line}}/E_{\text{cont}}^2$ appears inversely correlated with temperature showing a minimum at the observed temperature maximum. A turbulent velocity distribution peaking at ~ 10 km s⁻¹ has been deduced from the observed line-width temperature and the ratio $E_{\text{line}}/E_{\text{cont}}^2$.

Some confirmation of our results comes from a similar experiment performed on the same eclipse from an aircraft. Preliminary results by Keller (1982) show that line-width temperatures indicate a maximum closer to the limb than $2 R_\odot$ and perhaps even below $1.2 R_\odot$. Large turbulent velocity gradients need to be invoked to shift the maxima outward. For an unambiguous separation of thermal and turbulence broadening one would however have to await a successful Ly α temperature determination in the corona (Argo *et al.* 1982).

Acknowledgements

The authors are grateful to J. M. Pasachoff of Hopkins Observatory, Massachusetts, USA and the National Geographic Society for a timely supply of precalibrated film. The authors wish to thank Mrs. Jani for helping with the computations. The authors would also like to thank the two referees for their useful comments. The work was financially supported by the Department of Space, Government of India.

References

- Argo, H. V., Laros, J. G., Feldman, W. C., Beckers, J. M., Bruner, E. C. 1982, *Proc. Ind. Nat. Sci. Acad.*, **48**, Part A, 11.
- Bame, S. J., Asbridge, J. R., Feldman, W. C., Kearney, P. D. 1974, *Solar Phys.*, **35**, 137.
- Bates, B., Bradley, D. J., Kohno, T., Yates, H. W. 1966, *J. Sci. Instrum.*, **43**, 476.
- Brandt, J. C., Richard, W. M., Cassinelli, J. P. 1965, *Icarus*, **4**, 19.
- Brandt, S. 1970, in *Statistical and Computational Methods in Data Analysis*, Elsevier, p. **172**, 188.
- Chandrasekhar, T., Ashok, N. M., Desai, J. N., Vaidya, D. B., Angreji, P. D. 1980, *Bull. astr. Soc. India*, **8**, 87.
- Chandrasekhar, T., Desai, J. N., Angreji, P. D. 1981, *Appl. Opt.*, **20**, 2172.
- Desai, J. N., Chandrasekhar, T., Angreji, P. D. 1982, *J. Astrophys. Astr.*, **3**, 69.
- Dollfus, A. 1971, in *Proc. Physics of the Solar Corona*, Ed. C. J. Macris, D. Reidel, Dordrecht, p. 101.
- Jordon C. 1969, *Mon. Not. R. astr. Soc.*, **142**, 501.
- Keller, C. F. 1982, *Proc. Ind. Nat. Sci. Acad.*, **48**, Part A, 33.
- Kohl, J. L., Weiser, H., Withbroe, G. L., Noyes, R. W., Parkinson, W. H., Reeves, E. M., Munro,

- R. H., MacQueen, R. M. 1980, *Astrophys. J.*, **241**, L117.
- Kopp, R. A., Orrall, F. Q. 1976, *Astr. Astrophys.*, **53**, 363.
- Kuperus, M. 1969, *Space Sci. Rev.*, **9**, 713.
- Lieenberg, D. H., Bessey, R. J., Watson, B. 1975, *Solar Phys.*, **44**, 345.
- Mariska, J. T., Withbroe, G. L. 1978, *Solar Phys.*, **60**, 67.
- Nakada, M. P., Chapman, R. D., Neupert, W. M., Thomas, R. J. 1976, *Solar Phys.*, **47**, 611.
- Smartt, R. N., Ramsay, J. V. 1964, *J. Sci Instrum.*, **41**, 514.